International Journal of Nanomedicine

Dovepress
open access to scientific and medical research

Open Access Full Text Article

ORIGINAL RESEARCH

Efficient Colon Cancer Immunogene Therapy Through Co-Delivery of IL-22BP mRNA and Tumor Cell Lysate by CLSV Nanoparticles

Jing Huang[1,*], Kaiyu Wang[1,*], Xizi Fu[1,*], Manfang Zhu[2], Xiaohua Chen[1], Yan Gao[1], Pingchuan Ma[3], Xingmei Duan[2], Ke Men[1]

[1]State Key Laboratory of Biotherapy and Cancer Center, West China Hospital, Sichuan University, Chengdu, 610041, People's Republic of China; [2]Department of Pharmacy, Personalized Drug Therapy Key Laboratory of Sichuan Province Sichuan Academy of Medical Sciences & Sichuan Provincial People's Hospital, School of Medicine, University of Electronic Science and Technology of China, Chengdu, 610072, People's Republic of China; [3]State Key Laboratory of Oral Diseases & National Center for Stomatology & National Clinical Research Center for Oral Diseases & Department of Head and Neck Oncology, West China Hospital of Stomatology, Sichuan University, Chengdu, Sichuan, 610041, People's Republic of China

*These authors contributed equally to this work

Correspondence: Ke Men, State Key Laboratory of Biotherapy and Cancer Center, West China Hospital, Sichuan University, Chengdu, 610041, People's Republic of China, Email mendingbob@hotmail.com; Xingmei Duan, Department of Pharmacy, Personalized Drug Therapy Key Laboratory of Sichuan Province Sichuan Academy of Medical Sciences & Sichuan Provincial People's Hospital, School of Medicine, University of Electronic Science and Technology of China, Chengdu, 610072, People's Republic of China, Email duanxingmei2003@163.com

International Journal of Nanomedicine downloaded from https://www.dovepress.com/
For personal use only.

Background: Messenger ribonucleic acid (mRNA)-based gene therapy has great potential in cancer treatment. However, the application of mRNA-based cancer treatment could be further developed. Elevated delivery ability and enhanced immune response are advantages for expanding the application of mRNA-based cancer therapy. It is crucial that the prepared carrier can cause an immune reaction based on the efficient delivery of mRNA.

Methods: We reported DMP nanoparticle previously, which was obtained by the self-assembly of 1,2-dioleoyl-3-trimethylammonium propane (DOTAP) and (ethylene glycol)-*b*-poly (ε-caprolactone) (mPEG-PCL). Research demonstrated that DMP can deliver mRNA, siRNA, and plasmid. And it is applied to various tumor types. In our work, the tumor cell lysate was introduced to the internal DMP chain, fusing cell-penetrating peptides (CPPs) modification on the surface forming the CLSV system. And then mixed encoded IL-22BP (interleukin-22 binding protein) mRNA and CLSV to form CLSV/IL-22BP complex.

Results: The size of the CLSV system was 213.2 nm, and the potential was 45.7 mV. The transfection efficiency of the CLSV system is up to 76.45% in C26 cells via the micropinocytosis pathway. The CLSV system also could induce an immune response and significantly elevate the expression of CD80, CD86, and MHC-II in vivo. Then, by binding with IL-22BP (Interleukin-22 binding protein) mRNA, the CLSV/IL-22BP complex inhibited tumor cell growth, with an inhibition rate of up to 82.3% in vitro. The CLSV/IL-22BP complex also inhibited tumor growth in vivo, the tumor cell growth inhibition up to 75.0% in the subcutaneous tumor model, and 84.9% in the abdominal cavity metastasis tumor model.

Conclusion: Our work demonstrates that the CLSV system represents a potent potential for mRNA delivery.

Keywords: mRNA, cell-penetrating peptide, gene therapy, tumor cell lysate, immune response

Introduction

One of the main causes of death worldwide is cancer, with more than 9 million cancer-related deaths annually.[1] The third most common cancer is colon cancer which accounts for 10.2% of all cancer-related deaths worldwide.[2] Currently, conventional treatment methods for tumor disease include surgery, radiation therapy, and chemotherapy, each with unique limitations.[3,4] Gene therapy, defined as the introduction of therapeutic genes into cancer cells or tissues to cause cell death or slow cancer growth, has become a novel and effective method for cancer treatment.[5]

Received: 5 October 2023
Accepted: 20 December 2023
Published: 28 December 2023

© 2023 Huang et al. This work is published and licensed by Dove Medical Press Limited. The full terms of this license are available at https://www.dovepress.com/terms.php and incorporate the Creative Commons Attribution – Non Commercial (unported, v3.0) License (http://creativecommons.org/licenses/by-nc/3.0/). By accessing the work you hereby accept the Terms. Non-commercial uses of the work are permitted without any further permission from Dove Medical Press Limited, provided the work is properly attributed. For permission for commercial use of this work, please see paragraphs 4.2 and 5 of our Terms (https://www.dovepress.com/terms.php).

It has several advantages of mRNA-based gene therapy for cancer therapy.[6] For example, because of mRNA's lack of redundant gene sequence, it has increased transmission ability.[7] Moreover, the mRNA product was greatly increased due to it can translate into protein and does not need to enter into the nucleus.[8] At the same time, many mRNAs have entered clinical such as CV9202 and BNT162b1, demonstrating good therapeutic.[9,10] However, because the transfection rate and degradability limited the application. Therefore, it is crucial for the vector that not only further elevate the mRNA therapy potential but also confirm the mRNA integrality and deliver efficiency.

Peptide modification is one way to enhance mRNA delivery efficiency. CPPs peptide was known for its great penetrative abilities.[11] Research has reported that CPPs can deliver nucleic acid, protein, and compounds. However, the co-delivery of CPPs with vectors is a great challenge.[12] Importantly, The binding efficiency between carrier and CPPs should be ensured. Therefore, needs the carrier to have an appropriate site for modification. Moreover, CPPs binding with the vector will form steric hindrance, whether the steric hindrance influences the mRNA transfection ability hinges on the vector itself. This indicated that although CPPs modification further increases delivery efficiency, higher carrier requirements are needed.

Enhancing immune response-ability is another way to broaden the application of mRNA-based gene therapy called immunogene therapy. Immunogene therapy can efficiently elevate the anti-tumor immune response to inhibit cancer growth by introducing tumor antigens and cytokines.[13] The antigens expression on tumor cells can specifically arouse tumor immunoreaction.[14,15] Therefore, the tumor cell is ideal immune stimulators because they contain multitudinous antigens needed for immune activation.[16] Compared to tumor cells, lysate has more kinds of antigens such as membrane biomarkers, polysaccharides, and cytoplasmic proteins.[17] Tumor cell lysate has a great capacity for cancer immune therapy due to easy to obtain and short preparation time. However, it is inapposite for use alone in vivo because of the lysate's different solubilities, various charges, and heterogeneity. Due to the current mRNA delivery vector limited interspace. It is difficult to realize co-delivery lysate. Therefore, the carrier must possess enough interspace to encapsulate lysate based on high-efficiency delivery mRNA.

We previously reported DMP cationic nanoparticles, which were prepared by the DOTAP and mPEG-PCL self-assembly.[18] DMP nanoparticles are an ideal gene vector due to their simple structure and biodegradability.[19] And it can deliver different nucleic acids. Previous studies demonstrated that DMP was successfully applied in various tumor models.[18,19] IL-22BP, a soluble receptor of interleukin-22 (IL-22), is a member of the type II cytokine receptor family. Previous research has reported that IL-22 can bind to the IL-22R1 receptor to promote tumor cell proliferation.[20,21] As shown previously, IL-22BP binds with IL-22 to block the signal pathway of IL-22/IL-22R1, which indicated that IL-22BP is a potential tumor therapeutic target.[19] In this study, we sought to encapsulate tumor cell lysate onto the internal DMP nanoparticles and then modify it by fusing CPPs to form a CLSV system. Due to the CLSV system possessing CPPs and tumor cell lysate, it can realize the double purpose of mRNA delivery efficiency and elevate immune stimulation. We also characterize the CLSV system properties and mRNA delivery capacity in detail. By loading encoded IL-22BP mRNA to CLSV system to form CLSV/IL-22BP complex. We examined the ability to induce tumor apoptosis in vitro, before extending the research to investigate the tumor cell growth inhibition ability of the CLSV/IL-22BP complex in vivo.

Methods

Animals

All experiments on female Balb/C mice (6–8 weeks) were conducted under the guidance of the Animal Ethics Committee of the General Administration of Health of Sichuan University and the Standard Operating Procedures and Guidelines (SOP) for Experimental Animals of Sichuan University.

Cells

The C26 cells and 293T cells were purchased from ATCC, and cultured with Dulbecco Modified Eagle (DMEM) containing 10% fetal bovine serum (FBS, Cell Box, Chengdu).

Preparation and Characterization of Nanoparticles

The tumor cell lysate was prepared. Briefly, the C26 cells were digested with trypsin and used dulbecco's phosphate-buffered saline (DPBS) washed. Then oxidatively by hypochlorous acid for 30 min at 37°C. The sample was frozen and thawed 14–16 times before sonicating. Finally, use BCA method (Thermo, USA) detected the lysate concentration.

The CLSV system was synthesized based on the DMP nanoparticles. Briefly, DOTAP and mPEG-PCL were dissolved in dichloromethane at a mass ratio of 1:9. Rotary evaporation for 45 min to wipe out methylene dichloride followed by maleimide-PEG-PCL mixed with the sample. Then, the tumor cell lysate was added forming DMP-lysate nanoparticles. DMP-lysate and fused TAT-iRGD were dissolved in HEPES (50 mM) buffer at a mass ratio of 1:30 at 4°C overnight to form CLSV system, the amino acid sequence of TAT-iRGD is CRGDKGPDC-GRKKRRQRRRC. Using dynamic light scattering (Nano ZS, Malvern) measure the size and zeta potential of the DMP and CLSV system. Using transmission electron microscopy (TEM) observe the morphology of DMP and CLSV system.

mRNA Transcription in vitro

The IL-22BP mRNA was synthesized in vitro. Firstly, the PVAX1-IL-22BP plasmid DNA (pIL-22BP) as a template to generate the IL-22BP template. The pIL-22BP primer sequence was 5′-TAATACGACTCACTAT AGGGATGATGCCTAAGCATTGCCTTCTA GGTCTC-3′, and 5′-TTATCATGGAATGTGCACACATCTCTCCTTGCT -3′. Secondly, the T7 transcription kit (Thermo, USA) synthesizes mouse IL-22BP mRNA and then purifies it with a Clean-Up Kit (Thermo). The integrity of the obtained IL-22BP mRNA was analyzed using agarose gel.

RNase Protection Assay

The protective capacity of the CLSV on mRNA was analyzed. Free IL-22BP mRNA and CLSV/IL-22BP complex were treated with RNase A (0.25 mg/mL, Solarbio, Beijing) for 0 min, 15 min, 1 h, 2 h, and 4 h. Sodium dodecyl sulfate (0.24 mg/mL, SDS) were treated before samples subjected to electrophoresis.

Quantitative Real-Time PCR

CLSV/IL-22BP complex were transfected into C26 cells. After 72 h, total RNA was extracted and converted to cDNA using SuperScript II (Vazyme). Then, the cDNA was analyzed using the SYBR Green SuperMix kit (Vazyme). The IL-22BP and β-actin primer sequences are as follows: IL-22BP forward, 5′-ATTTTGCACTGGCAA GCAGG; reverse, 5′CCCTCCCGTAATACAGCTCG; and β-actin forward, 5′-CCCAGGCATTGCTGACA GG; reverse, 5′-TGGAAGGTGGCAG TGAGGC.

Cytotoxicity Assay

Using CCK-8 assay analysis the cytotoxicity of CLSV system in 293T cells. Series concentrations of CLSV and PEI25K were incubated with 293T cells for 24 h. The cytotoxicity of the treated cells was detected using a CCK-8 agent at 450 nm.

In vitro Transfection of the CLSV System

Using flow cytometer analysis the transfection ability of CLSV system. 293T and C26 were transfected EGFP mRNA by CLSV system (1:25, w/w) for 48 h. As transfection control, PEI25K/EGFP, DMP/EGFP, and DMP-CPPs/EGFP were used 1:1, 25:1, and 25:1 (w/w), respectively. The transfected C26 cells were detected.

Anti-Proliferation Assay

The growth inhibition ability of CLSV/IL-22BP was analyzed. The C26 cells were transfected with CLSV/IL-22BP complex for 96 h. The cells were imaged followed by CCK-8 agent treatment. Additionally, using 96-well plate seed C26 cells (100 cells/well). Subsequently, using 10 ng/mL IL-22 recombinant protein stimulation C26 cells every day for 5 days. After stimulation with IL-22 protein for 72 h, the CLSV/IL-22BP complex was transfected into C26 cells, the wells were imaged before the CCK-8 assay was added every day for 5 days.

Clonogenic Assay

Using clonogenic assay analysis the tumor cell growth inhibition capacity of CLSV/IL-22BP complex. Briefly, using 6-well plate seed C26 cells and treatment with the CLSV/IL-22BP complex. The transfected cells were cultured for 1–2 weeks to form colonies.

In vitro Apoptosis Assay

Using flow cytometry detect the apoptosis effect of CLSV/IL-22BP complex. Briefly, using 6-well plate seed C26 cells. The prepared cells were transfected with CLSV/IL-22BP complex for one day. The cells were dyed with apoptotic staining solution (Genechem, Shanghai, China) (Propidium Iodide and Annexin V).

Cellular Uptake Mechanism of the CLSV/mRNA Complex

Using flow cytometry and fluorescence microscopy detect the cellular uptake mechanism of the CLSV/IL-22BP complex. Briefly, using 6-well plate seed C26 cells for flow cytometry and chamber slides (Millicell) seed C26 cells for fluorescence microscopy. After 24 h, the cells were treated with serial inhibitors, including chlorpromazine (1 μg/mL), filipin III (1 mg/mL), amiloride (100 mM), wortmannin (10 mM), genistein (30 mM), and methyl-β-cyclodextrin (10 mM) for 0.5 h and then transfection by CLSV/IL-22BP complex for one day. The flow cytometry analyzed the cellular uptake efficiency. Additionally, the cells were stained with Hoechst (1 μg/μL, Solarbio) for nuclei acid and Dil (10 mg/mL, Beyotime) for the cell membrane. Fluorescence microscopy analysis.

In vitro Immunostimulation Experiments

The in vitro immunostimulation effect of the CLSV system was analyzed. Briefly, using BALB/c mice hindlimb bones extract BMDCs (bone marrow derived cells). The cells were cultured in RPMI 1640 medium for 5–7 days containing GM-CSF (20 ng/mL). To clarify whether the CLSV can be uptake by BMDCs, the Cy5.5-labeled CLSV (200 μg) was added to it for 24 h. Then, the cells were dyed with Hoechst for nuclei acid and Dio for cell membrane. Fluorescence microscopy analysis. Then, the immune response effect of the prepared CLSV was analyzed using flow cytometry. Briefly, lysate, DMP-CPPs, and CLSV were incubated with immature BMDCs on day 7. After 24 h, CD11c, CD80, CD86, and MHCII antibodies (BioLegend, USA) were used to stain the collected cells for 20 min before being analyzed by flow cytometry.

In vivo Immunostimulation Experiments

The in vivo immunostimulation effect of the CLSV system was analyzed. Briefly, lysate, DMP-CPPs, and CLSV system were intramuscularly injected in BALB/c for 24 h, 48 h, and 72 h, respectively. The lymph nodes (LN) and spleen were collected to extract single lymphocytes. The prepared cells were stained with CD11c, CD80, CD86, and MHCII antibodies (BioLegend, USA) for 20 min before being analyzed by flow cytometry.

Tumor Inhibition Assay in vivo

The tumor inhibition ability of the CLSV/IL-22BP was analyzed in BALB/c female mice. To establish an abdominal cavity metastatic model, the C26 tumor cells were intraperitoneal injection at a concentration of 2×10^5 cells per mouse. The model mice received intraperitoneal injections of normal saline (NS), CLSV system, and CLSV/IL-22BP (10 μg) complex for 10 treatments every day. On day 13, the tumors, kidney, spleen, liver, heart, and lung were collected and soaked in paraformaldehyde.

The subcutaneous model was established by subcutaneous injection of C26 tumor cells at a concentration of 2.5×10^6 cells per mouse. The model mice received subcutaneous injections of normal saline (NS), CLSV system, and CLSV/IL-22BP (10 μg) complex for 13 treatments every day. On day 16, the tumors, kidney, spleen, liver, heart, and lung were collected and soaked in paraformaldehyde.

Immunohistochemical Analysis

The protein expression in tumor tissue was analyzed using immunological reactions. The hematoxylin-eosin (HE) stain assay to visualize cellular structures. The TUNEL (Madison, WI, USA) assay for apoptosis was detected. The

immunohistochemical assay for the specific antibodies against IL-22BP, CD8, IFN-γ, mannose receptor, TNF-α, CD80, and CD31 (Abcam) at 4°C overnight.

Blood Tests

CLSV systems were intravenously injected into female BALB/c mice for 24 h. Peripheral blood was collected and using diverse indices detected. Moreover, serum was collected using a series of components analyzed.

Statistical Analysis

Using GraphPad statistically analyze the data by *t*-tests or one-way ANOVA. The data are shown as the mean ± standard deviation (SD). The statistical significance was defined when $P < 0.05$.

Results

Preparation and Characterization of the CLSV/mRNA Complex

In our research, the DMP nano-backbone is the skeleton of the CLSV system. The CLSV system was constructed by tumor cell lysate encapsulated into the internal DMP chain, and the fused CPPs (TAT-iRGD) were modified on the surface. Then the CLSV system binds with IL-22BP mRNA forming the CLSV/ IL-22BP complex (Figure 1A).

We then measured the diameter and potential of the DMP and CLSV system. The average diameter of prepared DMP and CLSV system were 28.8 nm and 213.2 nm (Figure 1B), respectively. According to our results, the average ζ-potential of DMP and CLSV system were 44.6 mV and 45.7 mV, respectively (Figure 1E). Then, we used TEM to further observe the morphologies of prepared DMP and CLSV systems. (Figure 1C and D). We used 293T cells to analyze the

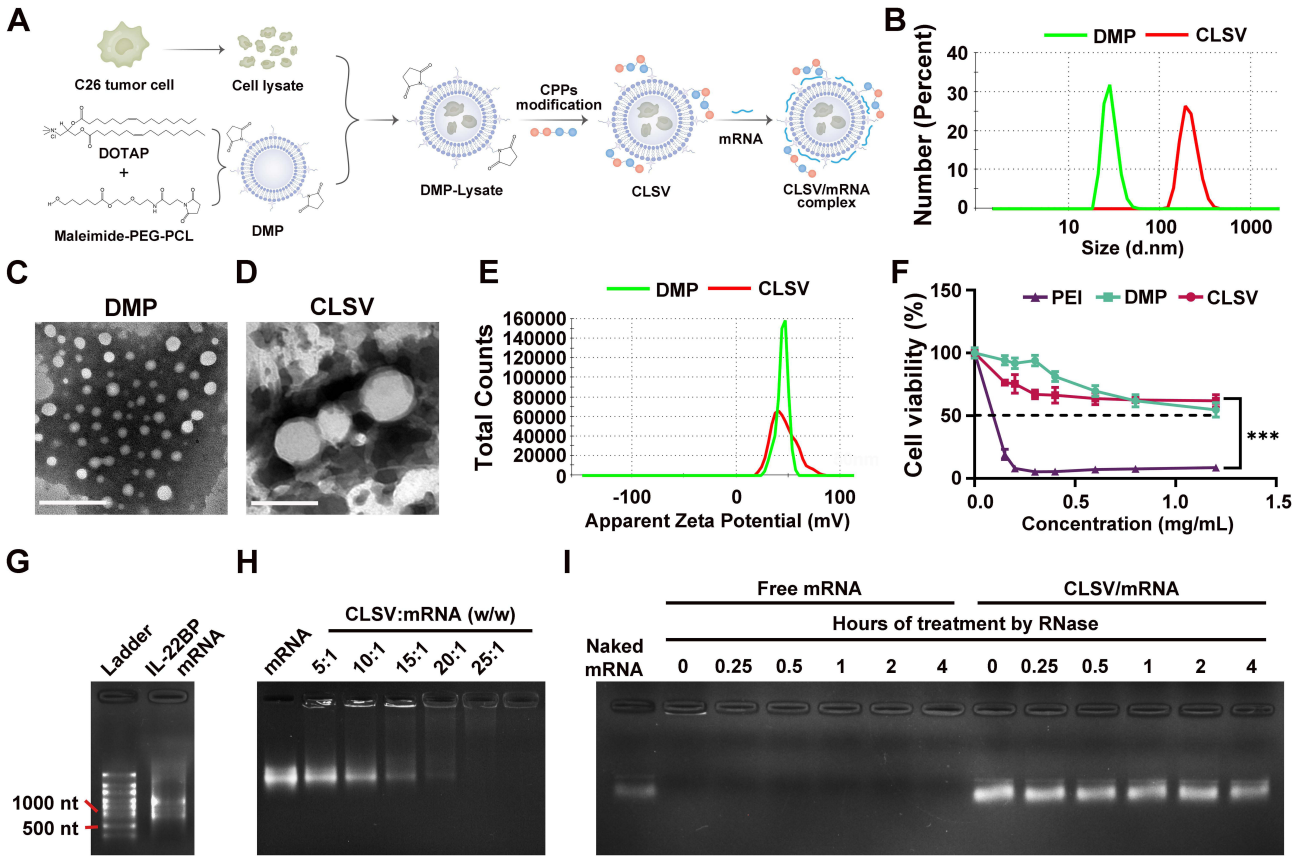

Figure 1 Preparation and characterization of the CLSV system. (**A**) CLSV/IL-22BP complex synthesis. (**B**) Size of DMP and CLSV system. (**C**) TEM of DMP (scale bar: 200 nm). (**D**) TEM of CLSV system (scale bar: 200 nm). (**E**) Zeta potential of DMP and CLSV system. (**F**) Cell toxicity of PEI25K, DMP, and CLSV system in 293T cells (***P < 0.001). (**G**) Electrophoresis analysis IL-22BP mRNA. (**H**) Electrophoresis analysis gel retarding effect of CLSV system to mRNA. (**I**) Electrophoresis analysis RNase protects the effect of the CLSV system on mRNA.

cytotoxicity of the DMP and CLSV system. According to our results, the IC50 of the DMP and CLSV system was>1.2 mg/mL, which was much higher than PEI25K (< 0.2 mg/mL) (Figure 1F). These results indicated that the CLSV had far lower toxicity than PEI25K. Then, the integrality of synthesized IL-22BP mRNA was confirmed using agarose gel electrophoresis. According to our result, the result demonstrated a band close to 690 nucleotides, the length in accord with the expected IL-22BP mRNA (Figure 1G). Then, the CLSV/IL-22BP complex was prepared by incubation of mRNA and positive charge CLSV. The binding capacity of the CLSV was investigated. According to our results, the mRNA band was almost invisible when the mass ratio of CLSV to mRNA was 25:1 (Figure 1H). These results indicated that mRNA was completely bound to CLSV. Moreover, as shown in Figure 1I, the protected mRNA by the CLSV system against RNase up to 4 h. Compared to the CLSV/IL-22BP complex, the naked mRNA was entirely invisible within 15 min, indicating it was degraded fully. These results suggested that the CLSV system could efficiently bind with mRNA.

In vitro Transfection Study

The delivery ability of mRNA by CLSV was analyzed in vitro. The DMP-CPPs and CLSV system efficiency deliver EGFP-encoded mRNA into 293T cells (Figure 2A). Additionally, after treatment with PEI25K, the 293T cells were rounded and a dirty background was observed, demonstrating PEI25K cytotoxicity. Compared to PEI25K, although a larger mass ratio was used in the CLSV system, more normal cell morphology was performed. Then, we detected the transfection rate of the CLSV/mRNA complex and DMP-CPPs. As shown in Figures 2B and S1A, after the CLSV/mRNA complex and DMP-CPPs were treated, the transfection efficiency was up to 87.43% ± 1.1% and 83.01% ± 0.3%, while the DMP and PEI25K were decreased to 78.84% ± 1.0% (P < 0.001) and 70.88% ± 1.7% (P < 0.001). Our result

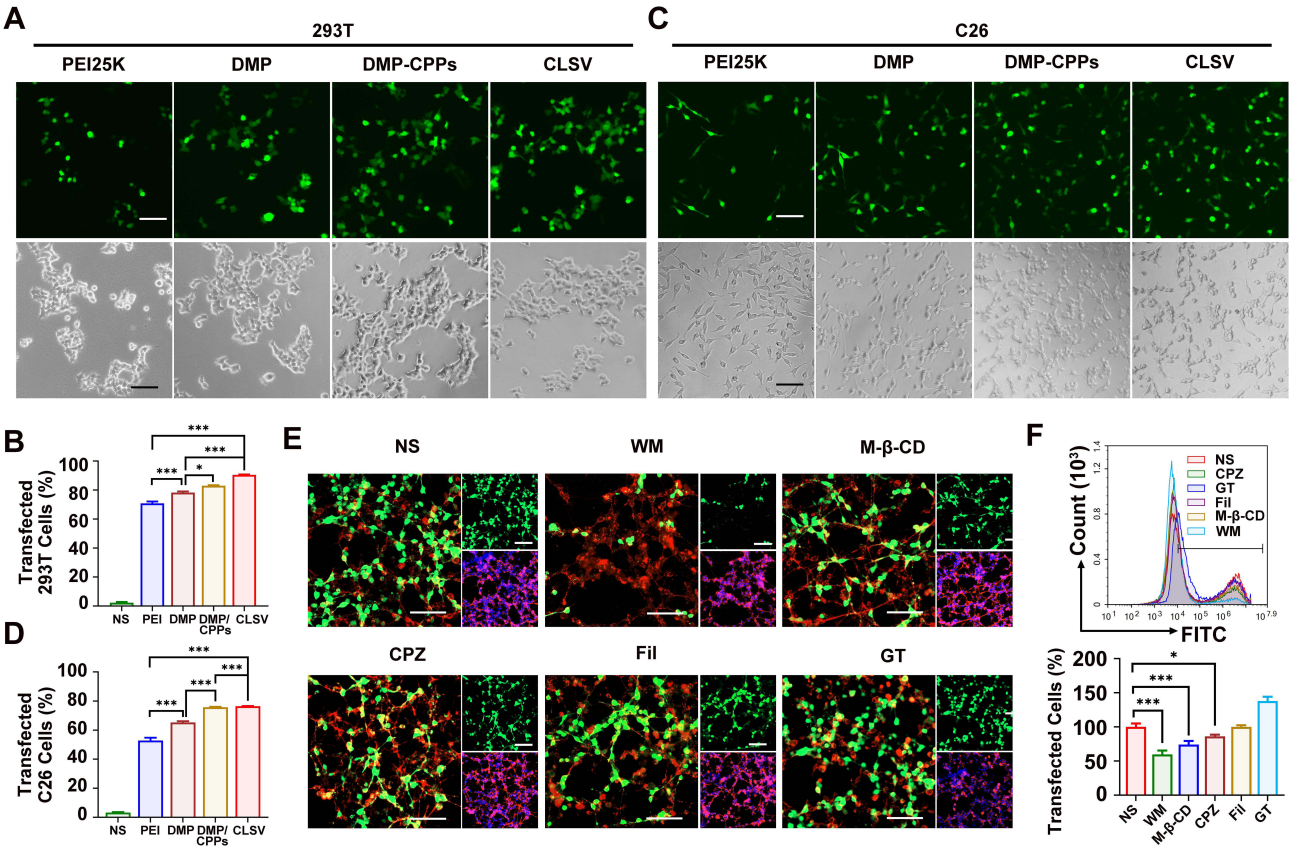

Figure 2 In vitro transfection study. (**A**) Fluorescence images analysis of the transfection rate of CLSV/IL-22BP complex in 293T cells (scale bar: 100 μm). (**B**) Flow cytometry analysis of the transfection rate of CLSV/IL-22BP complex in 293T cells (*P < 0.05, ***P < 0.001). (**C**) Fluorescence images analysis of the transfection rate of CLSV/IL-22BP complex in C26 cells (scale bar: 100 μm). (**D**) Flow cytometry analysis of the transfection rate of CLSV/IL-22BP complex in C26 cells (***P < 0.001). (**E**) Fluorescent images analyze the uptake rate of different inhibitors (scale bar: 100 μm). (**F**) Flow cytometry analysis of the uptake rate of different inhibitors (*P < 0.05, ***P < 0.001).

demonstrated that the delivery ability was elevated after CPPs modification, and there is no significant difference between CLSV and DMP-CPPs, indicating that there is no effect of transfection efficiency after encapsulated lysate into the DMP chain. Additionally, the CLSV system delivery ability was also analyzed in C26 cells. According to our result, observed cell damage and shrinking after PEI25K stimulation (Figure 2C). This result demonstrates stronger toxicity of PEI25K in C26 cells. The transfection rate was detected. As shown in Figures 2D and S1B, the transfection rate was up to 76.45 ± 0.4% and 75.75% ± 0.4% in the CLSV group and DMP-CPPs group, while the transfection of DMP and PEI25K was 65.30% ± 1.2% ($P < 0.01$) and 52.8% ± 2.7% ($P < 0.01$). These results suggested that mRNA can be high-efficiency and lower toxicity delivered by the CLSV system in vitro.

The uptake mechanism of the CLSV/IL-22BP complex was further investigated. Research demonstrated that caveolin-mediated endocytosis, micropinocytosis, lipid raft-mediated endocytosis, and clathrin-mediated endocytosis the currently endocytosis internalization mechanisms.[22,23] Before transfection, the cells were stimulated by series inhibitors, including genistein (GT) and filipin III (Fil) for caveolin-mediated endocytosis, wortmannin (WM) for micropinocytosis, methyl-β-cyclodextrin (M-β-CD) for lipid raft-mediated endocytosis, and chlorpromazine (CPZ) for clathrin-mediated endocytosis.

As shown in Figure 2E, after WM treatment, the efficiency was significantly reduced. Moreover, the transfection rate was detected. As shown in Figure 2F, after WM treatment, the transfection rate reduced to 40.25% ($P < 0.001$) (Figure 2F), indicating micropinocytosis played a main role in the intake of the CLSV/IL-22BP complex in C26 cells.

CLSV System Efficiently Activated the Immune Response in vitro and in vivo

The immune stimulation capacity of the CLSV was investigated. Previous research demonstrated that DCs play a key role in antigen presentation.[24] The intake effect of the CLSV system by BMDCs was analyzed first. We incubated the Cy5.5-labeled CLSV system with BMDCs for 24 h. As shown in Figure 3A, the Cy5.5-labeled CLSV system had obvious uptake into BMDCs. Then, the effect of DC maturation was investigated after CLSV system stimulation, and the expression of matured BMDCs was investigated. In the NS group, the percentage of $CD11c^+$ $CD80^+$ $CD86^+$ was 8.0% ± 0.4%. While in the DMP group, lysate group, and CLSV group, the expression respectively was 36.8% ± 0.6%, $P < 0.001$, 37.6% ± 0.8%, $P < 0.001$, and 57.6% ± 1.8%, $P < 0.001$ (Figure 3B). These results demonstrated that CLSV could highest efficiency induce BMDC maturation. In the process of antigen presentation, it is important for MHC expression.[25] Therefore, we studied the expression of MHC. As shown in Figure 3C, in the NS group, the percentage of $CD11c^+$ $MHC\text{-}II^+$ was 25.4% ± 1.4%, while in the DMP group, lysate group, and CLSV group, the expression respectively was 34.6% ± 2.5%, 42.1% ± 1.0% ($P < 0.01$), and 62.5% ± 1.7% ($P < 0.001$). These results showed that the empty DMP nanoparticles could lead to the maturation of DCs. Additionally, although the expression of DCs was elevated by lysate alone, it was ulteriorly enhanced after CLSV system treatment. And the immune response of the CLSV system ulteriorly increases, indicating an adjuvant-like ability of DMP. In a word, these results demonstrated that the DCs can be efficiently activated and maturation by the CLSV system in vitro.

Then, we analyzed the immune response effect of the CLSV nanoparticles in vivo. DMP, lysate, and CLSV system were intramuscular injection, and relative expression in LNs and spleen were monitored at 24 h, 48 h, and 72 h. The LNs were monitored first. As shown in Figure 3D, the expression of $CD11c^+$, $CD11c^+$ $CD80^+$, $CD11c^+$ $CD86^+$, and $CD11c^+$ $MHC\text{-}II^+$ in the CLSV system group were 52.8% ± 0.4% (48 h), 74.5% (48 h), 68.4% (48 h), and 79.4% (72 h), respectively. In the spleen, we monitor similar biomarker expression. As shown in Figure 3E, the expression of $CD11c^+$, $CD11c^+$ $CD80^+$, $CD11c^+$ $CD86^+$, and $CD11c^+$ $MHC\text{-}II^+$ in the CLSV system group were 55.2% ± 1.5% (48 h), 52.2% ± 0.8% (48 h), 37.8% ± 1.6% (48 h), and 29.0% ± 2.0% (48 h), respectively. Consistent with the in vitro results, empty DMP nanoparticles also led immune stimulation response in vivo. These results further demonstrated the limited immune response of lysate injection alone. Additionally, the effect of immune response was elevated after lysate was introduced into the DMP skeleton. Which indicates an adjuvant-like ability of DMP. In summary, these results demonstrated that the DCs can be efficiently maturation and activation by the CLSV system, suggesting the potent immune therapeutic ability in vivo.

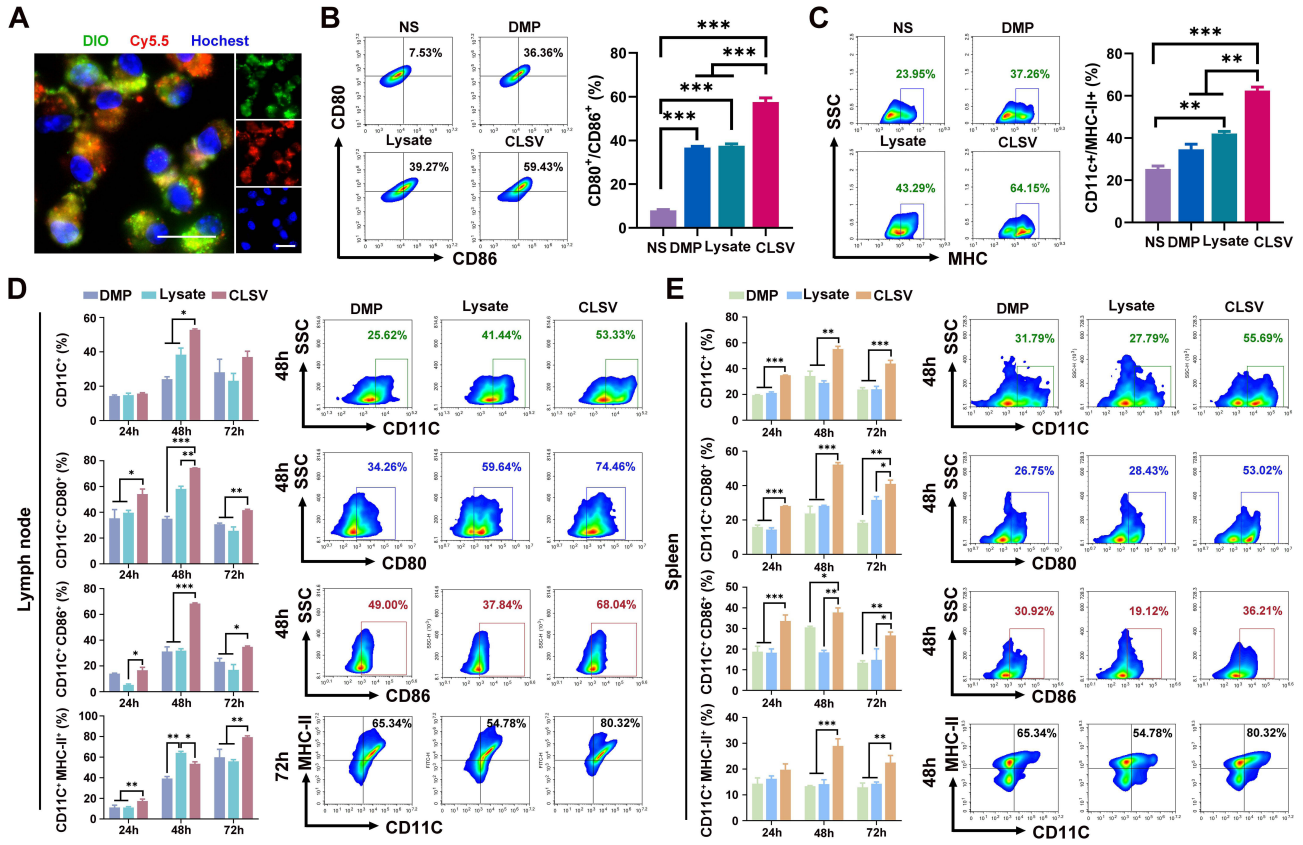

Figure 3 CLSV system efficiently activated the systemic immune response in vitro and in vivo. (**A**) Fluorescent image analysis of the CLSV system uptake by BMDCs (scale bar: 20 μm). (**B**) Flow cytometry analysis of the expression of $CD11c^+$ $CD80^+$ $CD86^+$ in BMDCs (***P < 0.001). (**C**) Flow cytometry analysis of the expression of $CD11c^+$ $MHC\text{-}II^+$ in BMDCs (**P < 0.01, ***P < 0.001). (**D**) Flow cytometry analysis the expression of $CD11c^+$, $CD80^+$, $CD86^+$, and $MHC\text{-}II^+$ in LNs (*P < 0.05, **P < 0.01, ***P < 0.001). (**E**) Flow cytometry analysis the expression of $CD11c^+$, $CD80^+$, $CD86^+$, and $MHC\text{-}II^+$ in LNs (*P < 0.05, **P < 0.01, ***P < 0.001).

CLSV/IL-22BP mRNA Complex Suppressed C26 Cell Proliferation in vitro

IL-22BP, a member of the type II cytokine receptor family, can block the IL-22/IL-22R1 signaling pathway via competitively binding to IL-22, inhibiting cancer cell growth (Figure 4A). Firstly, we detected the delivery ability of IL-22BP mRNA by the CLSV system in C26 cells. The RNA expression of IL-22BP was 2.5×10^4-fold higher than the NS group after the CLSV/IL-22BP complex was transfected (Figure 4B). As shown in Figure 4C, the protein concentration of IL-22BP was 310 pg/mL in the C26 supernatant after CLSV/IL-22BP complex transfection. These results indicated that the CLSV system can highly efficiently transfected IL-22BP mRNA into cells and can further translate it into IL-22BP protein.

Then, the proliferation inhibitory effect of the CLSV/IL-22BP complex in C26 cells was studied in vitro. Previous studies reported that IL-22 can promote cancer cell proliferation via binding with IL-22R1, which can be blocked by IL-22BP. We then investigated the tumor inhibition effect of IL-22BP. The growth was restrained after transfection by the CLSV/IL-22BP complex (Figure 4D), resulting in a 95.3% ± 0.9% ($P < 0.001$) inhibition rate (Figure 4E). Moreover, we studied the proliferation effect of IL-22 cytokines. As shown in Figure S2A, the C26 cells showed obvious proliferation after IL-22 cytokines treatment. As shown in the CCK-8 assay, compared to the NS group, on days 2, 3, 4, and 5, the confluency of C26 cells increased by 152.7% ± 32.3% ($P < 0.05$), 193% ± 18.6% ($P < 0.001$), 223.5% ± 3.4% ($P < 0.001$), and 317.7% ± 6.2% ($P < 0.001$), respectively, in a time-dependent manner (Figure S2B). Importantly, the uptrend was inhibited after transfection with the CLSV/IL-22BP complex (Figure 4F), and the confluence decreased from 317.7% to 29.8% ($P < 0.001$) on day 5 (Figure 4G), these results indicated that the proliferation effect of IL-22 can be neutrally by IL-22BP. At the same time, the inhibition ability of tumor cell proliferation of CLSV/IL-22BP complex was further confirmed via clonogenic assay. After being transfected by the CLSV/IL-22BP complex, the growth clones were

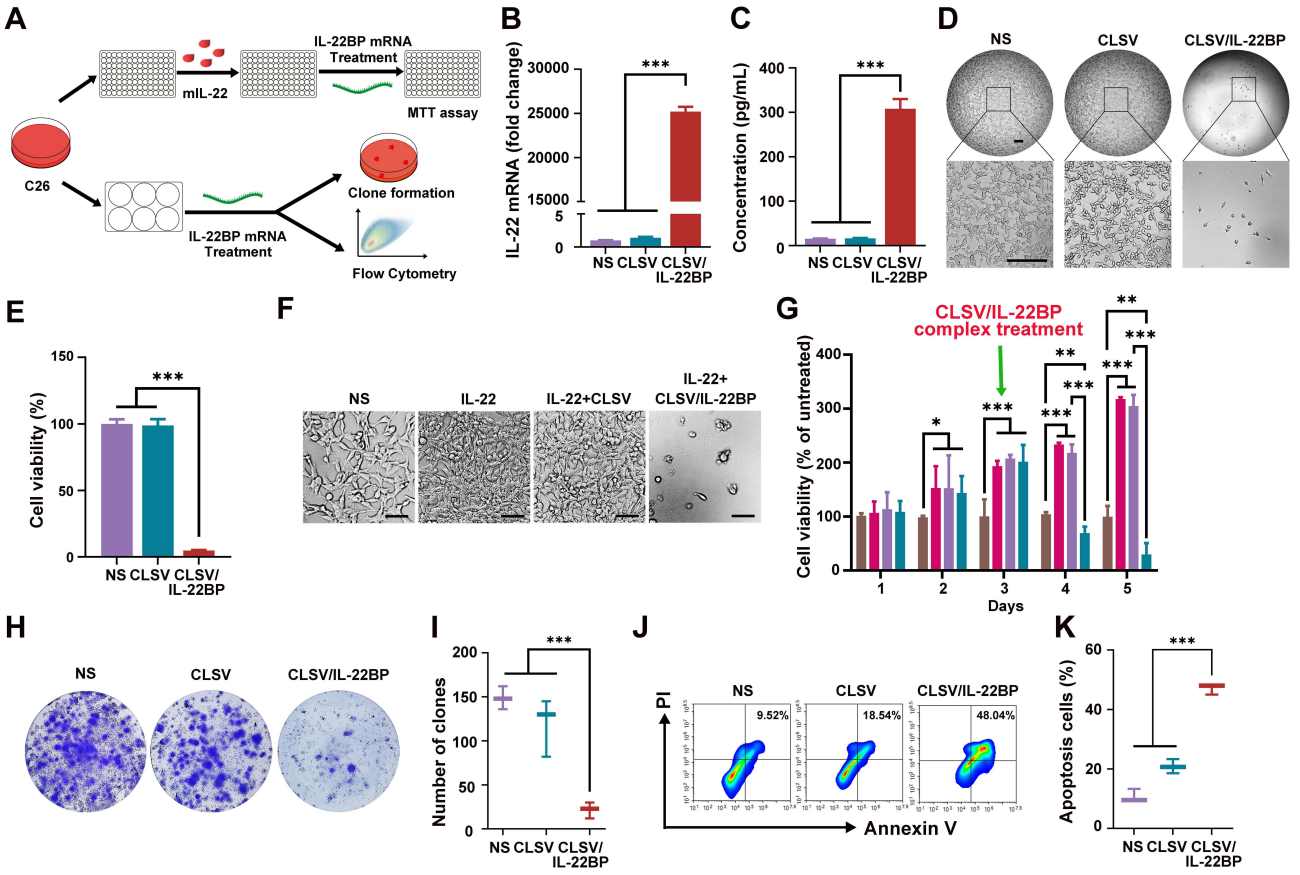

Figure 4 CLSV/IL-22BP complex inhibited C26 cell proliferation in vitro. (**A**) The experimental design of CLSV/IL-22BP complex in C26 cells. (**B**) Q-PCR analysis of the expression of IL-22BP mRNA in C26 cells (***P < 0.001). (**C**) ELISA analysis of the expression of IL-22BP protein in C26 cells supernatant (***P < 0.001). (**D**) Images analysis of the proliferation-inhibition effect of CLSV/IL-22BP complex (scale bar: 200 μm). (**E**) MTT analysis of the proliferation-inhibition effect of CLSV/IL-22BP complex (***P < 0.001). (**F**) Images analysis of the proliferation-promoting effect of IL-22 and neutralized by CLSV/IL-22BP complex (scale bar: 100 μm). (**G**) MTT analysis of the proliferation-promoting effect of IL-22 and neutralized by CLSV/IL-22BP complex (*P < 0.05, **P < 0.01, ***P < 0.001). (**H** and **I**) Clonogenic assay analysis of the proliferation-inhibition effect of CLSV/IL-22BP complex (***P < 0.001). (**J** and **K**) Flow cytometry analysis of the apoptosis effect of CLSV/IL-22BP complex (***P < 0.001).

significantly decreased (Figure 4H). As shown in Figure 4I, the clone numbers were decreased to 28 ± 7 after CLSV/IL-22BP complex treatment. According to our result, the inhibition rate was 82.3% ± 7.1% (P < 0.001) in the CLSV/IL-22BP complex group (Figure S2C). However, in comparison with the CLSV/IL-22BP group, the clone number of the NS group was 119 ± 27, and the DMP group was 149 ± 11 (Figure 4I), indicating IL-22BP can highly inhibit the proliferation of C26 cells.

Additionally, the apoptosis effect of CLSV/IL-22BP was further studied in C26 cells. According to our result, the apoptotic rate of C26 cells was obviously increased after CLSV/IL-22BP transfected, with an apoptotic cell rate of up to 47.1% ± 1.5% (Figure 4J), while the rates in the DMP and CLSV system groups were 20.8% ± 1.9% (P < 0.001) and 10.7% ± 1.8% (P < 0.001), respectively (Figure 4K). In summary, our results indicated that IL-22BP exerts an anti-cancer effect through preventing the IL-22/IL-22R1 signaling axis and inducing apoptosis to inhibit cell growth.

CLSV/IL-22BP Complex Efficiently Inhibited Tumor Growth in vivo

The CLSV/IL-22BP complex tumor growth inhibition effect was further investigated in vivo. First, we use the abdominal cavity metastatic model to confirm the therapeutic efficacy (Figure 5A). According to our results, compared to the NS group, the CLSV/IL-22BP complex group showed fewer metastatic tumor nodules (yellow arrows) (Figure 5B). Additionally, obvious blood-like ascites developed in the NS group, indicating serious tumor infiltration. Meanwhile, CLSV/IL-22BP complex-treated mice showed an obvious decrease in ascites volume. The volume decreased to 0.25 ± 0.63 mL in the CLSV/IL-22BP complex group (Figure 5C). Compared to the CLSV/IL-22BP complex group, the ascites

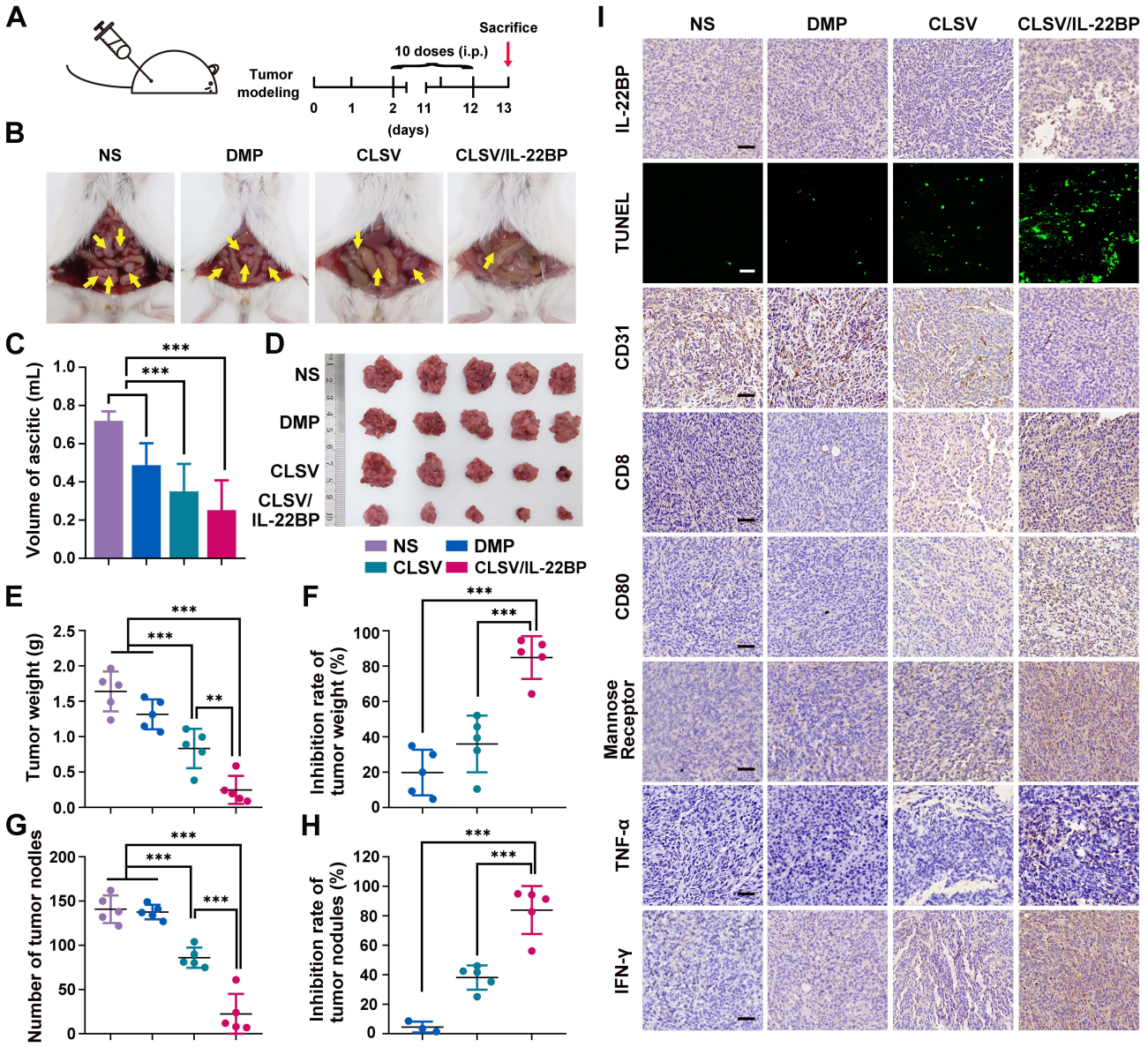

Figure 5 The CLSV/IL-22BP complex inhibited abdominal cavity metastatic tumor growth in vivo. (**A**) The experimental plan of CLSV/IL-22BP complex in abdominal cavity metastatic tumor model. (**B**) Images of representative mice from each group. (**C**) Average ascitic volume from each group (***P < 0.001). (**D**) Image of collected tumor nodules from each group. (**E**) Average tumor weight of collected tumor nodules from each group (**P < 0.01, ***P < 0.001). (**F**) Inhibition rate of tumor weight from each group (***P < 0.001). (**G**) Average tumor nodules of collected tumor nodules from each group (***P < 0.001). (**H**) Inhibition rate of tumor nodules from each group (***P < 0.001). (**I**) Immunohistochemical analysis relative protein expression in tumor tissue (scale bars: 50 μm).

volume in the CLSV group was 0.35 ± 0.59 mL, in the DMP group was 0.49 ± 0.43 mL (P < 0.001), and in the NS group was 0.72 ± 0.14 (Figure 5C). Then, we extract the tumor nodules. As shown in Figure 5D, after CLSV/IL-22BP complex treatment, the average number of nodules was less than in other groups, and the tumor weight was 0.25 ± 0.35 g. Lighter than other groups such as the CLSV group, DMP group, and NS group were 0.83 ± 0.53 g, 1.32 ± 0.35 g, and 1.64 ± 0.52 g, respectively. (Figure 5E). Resulting 84.9% ± 21.6% inhibition rate in the CLSV/IL-22BP complex group (Figure 5F). Similarly, after CLSV/IL-22BP complex treatment, the number of tumor nodules decreased to 22 ± 43, while the CLSV, DMP, and NS groups were 86 ± 21, 138 ± 15, and 141 ± 25, respectively (Figure 5G). Resulted in an 83.9% ± 30.8% inhibition effect in the CLSV/IL-22BP group (Figure 5H). In a word, these results indicated that the CLSV/IL-22BP complex can effectively suppress tumor cell proliferation in abdominal cavity metastases.

Then, the CLSV/IL-22BP complex therapy mechanism was further analyzed by immunohistochemical analyses. According to our results, compared to the NS groups, there was a significantly elevated expression of IL-22BP after CLSV/IL-22BP complex treatment (Figure 5I). According to the results of the TUNEL assay, after CLSV/IL-22BP complex treatment, the apoptosis effect was significantly increased (Figure 5I). Additionally, compared to other groups, staining with CD31 revealed that the microvessel density was significantly decreased following treatment with the CLSV/IL-22BP complex, indicating an anti-angiogenesis effect of the CLSV/IL-22BP complex (Figure 5I). The CLSV/IL-22BP complex was also found to enhance immune cell infiltration, with increased levels of CD8, CD80, TNF-α, IFN-γ, and mannose receptor markers following treatment with the CLSV/IL-22BP complex, demonstrating the ability to activate and recruit T cells, macrophages, and monocytes (Figure 5I). These results further indicate that the immune response was initiated following CLSV/IL-22BP complex treatment. Moreover, as shown in Figure 6A, there are no obvious pathological injuries in main organs via HE analysis, which suggestion that the high safety of the CLSV/IL-22BP complex in vivo. In summary, our results indicated that the CLSV/IL-22BP complex could induce anti-apoptosis, angiogenesis, and immune response to inhibit the tumor cell growth in vivo.

Additionally, the CLSV/IL-22BP complex tumor growth inhibition effect in the subcutaneous tumor model was also studied (Figure 7A). According to our results, the tumor volume was measured every day, and the tumors were extracted at the endpoint, the results showed that the CLSV/IL-22BP complex exerted an antitumor effect (Figure 7B and C). After CLSV/IL-22BP complex treatment, the average tumor volume decreased to 176.4 ± 46.7 mm^3 (Figure 7D). Compared to the CLSV/IL-22BP complex group, the tumor volume in the CLSV group, DMP group, and NS group were 382.8 ± 161.9 mm^3 ($P < 0.05$), 515.1 ± 150.6 mm^3 ($P < 0.001$), and 705.3 ± 132.4 mm^3 ($P < 0.001$), respectively. As shown in Figure 7E, after CLSV/IL-22BP complex treatment, there was a lighter tumor weight of 0.15 ± 0.07 g. Compared to the CLSV/IL-22BP complex group, the tumor weight in the CLSV group was 0.36 ± 0.16 g, in the DMP group was 0.49 ± 0.23 g, and NS group was 0.57 ± 0.30 g, with a 75.0% ± 5.9 inhibition rate after CLSV/IL-22BP complex treatment (Figure 7F). In summary, our results demonstrated the high inhibition effect of the CLSV/IL-22BP complex in vivo.

Then, the therapy mechanism of the CLSV/IL-22BP complex was further analyzed by immunohistochemical analyses. According to our results, compared to the NS groups, the expression of IL-22BP was increased after CLSV/IL-22BP complex treatment (Figure 7G). According to the results of the TUNEL assay, after CLSV/IL-22BP complex treatment, the apoptosis effect was significantly increased (Figure 7G). Moreover, compared to the other groups, the microvessel density was significantly decreased in the CLSV/IL-22BP complex group, as determined by CD31 staining, indicating that the CLSV/IL-22BP complex induced anti-angiogenesis effects (Figure 7G).

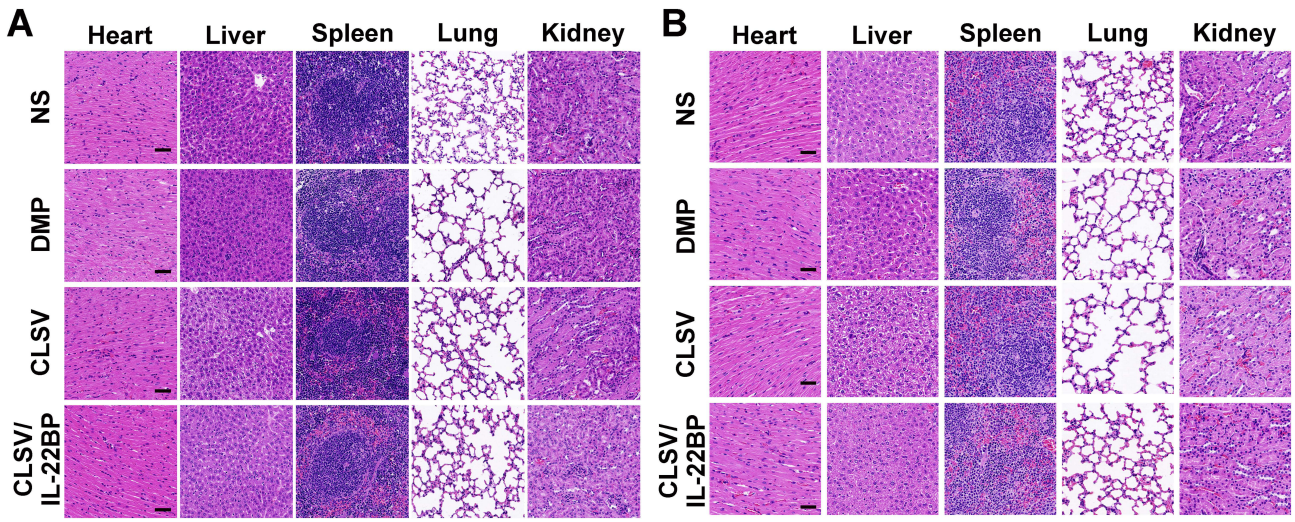

Figure 6 HE analysis in vivo. (**A**) HE analysis of the main organ morphology in the C26 abdominal cavity metastatic model (scale bars: 50 μm). (**B**) HE analyzed the main organ morphology in the C26 subcutaneous model (scale bars: 50 μm).

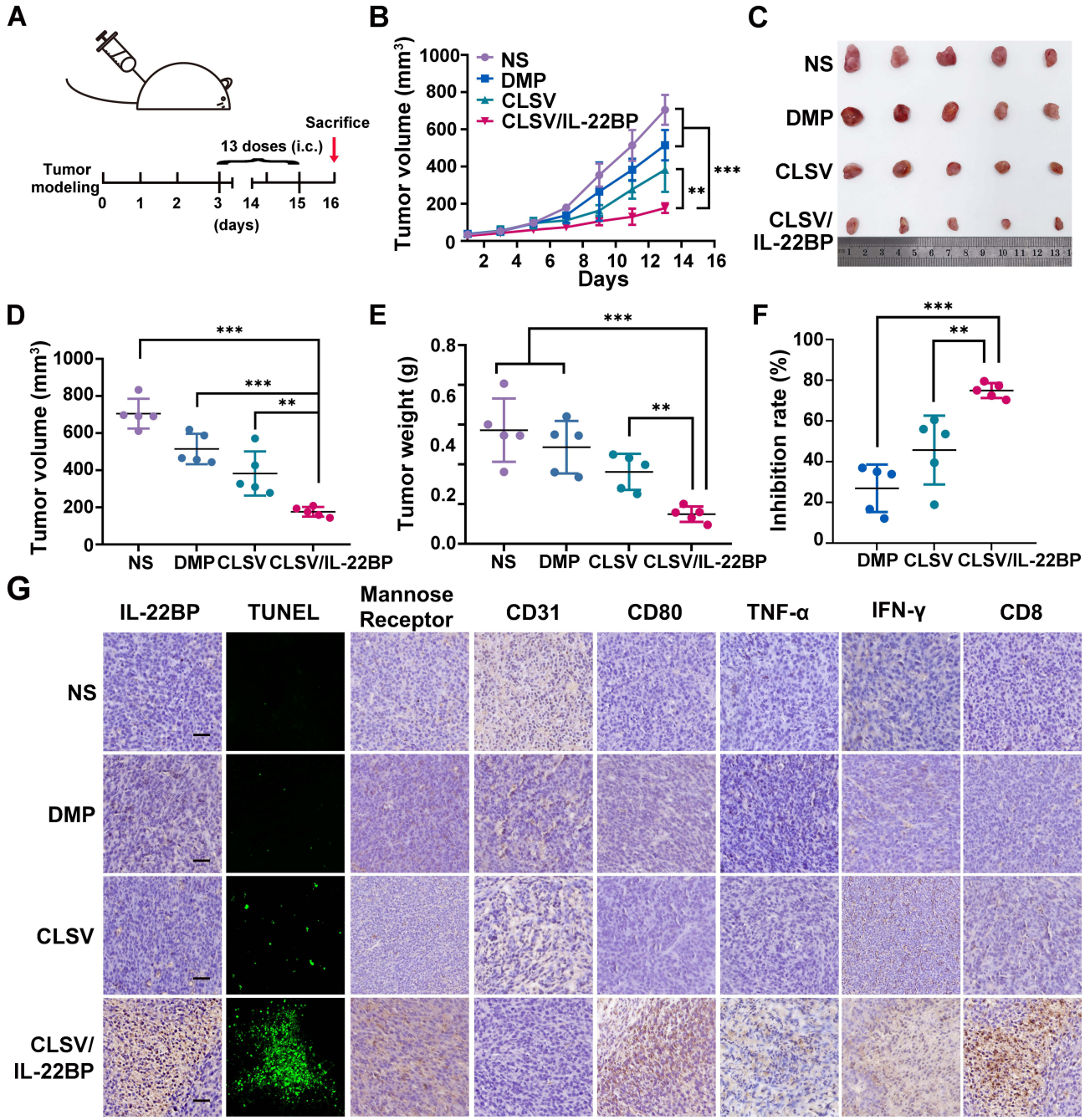

Figure 7 CLSV/IL-22BP complex suppressed the C26 subcutaneous xenograft model in vivo. (**A**) The experimental plan of CLSV/IL-22BP complex in subcutaneous model. (**B**) Tumor growth curve from each group (**P < 0.01, ***P < 0.001). (**C**) Image of collected tumors from each group. (**D**) Average tumor volume from each treatment group in the endpoint (**P < 0.01, ***P < 0.001). (**E**) Average tumor weight from each group (**P < 0.01, ***P < 0.001). (**F**) Inhibition rate of tumor weight from each group (**P < 0.01, ***P < 0.001). (**G**) Immunohistochemical analysis relative protein expression in tumor tissue (scale bars: 50 μm).

The CLSV/IL-22BP complex was also shown to enhance immune cell infiltration, as demonstrated by increased levels of CD8, CD80, TNF-α, IFN-γ, and mannose receptor markers following treatment with the CLSV/IL-22BP complex, demonstrating the recruit T cells ability, macrophages, and monocytes (Figure 7G). These results further indicate that the immune response was initiated during CLSV/IL-22BP complex treatment. Moreover, as shown in Figure 6B, there are no obvious pathological injuries in main organs via HE analysis, which suggestion that the high safety of the CLSV/IL-22BP complex in vivo. Additionally, the blood analysis demonstrated that there is no obvious toxicity, and the CLSV system intravenously injection has no influence on the liver and kidney (Figure 8). In summary,

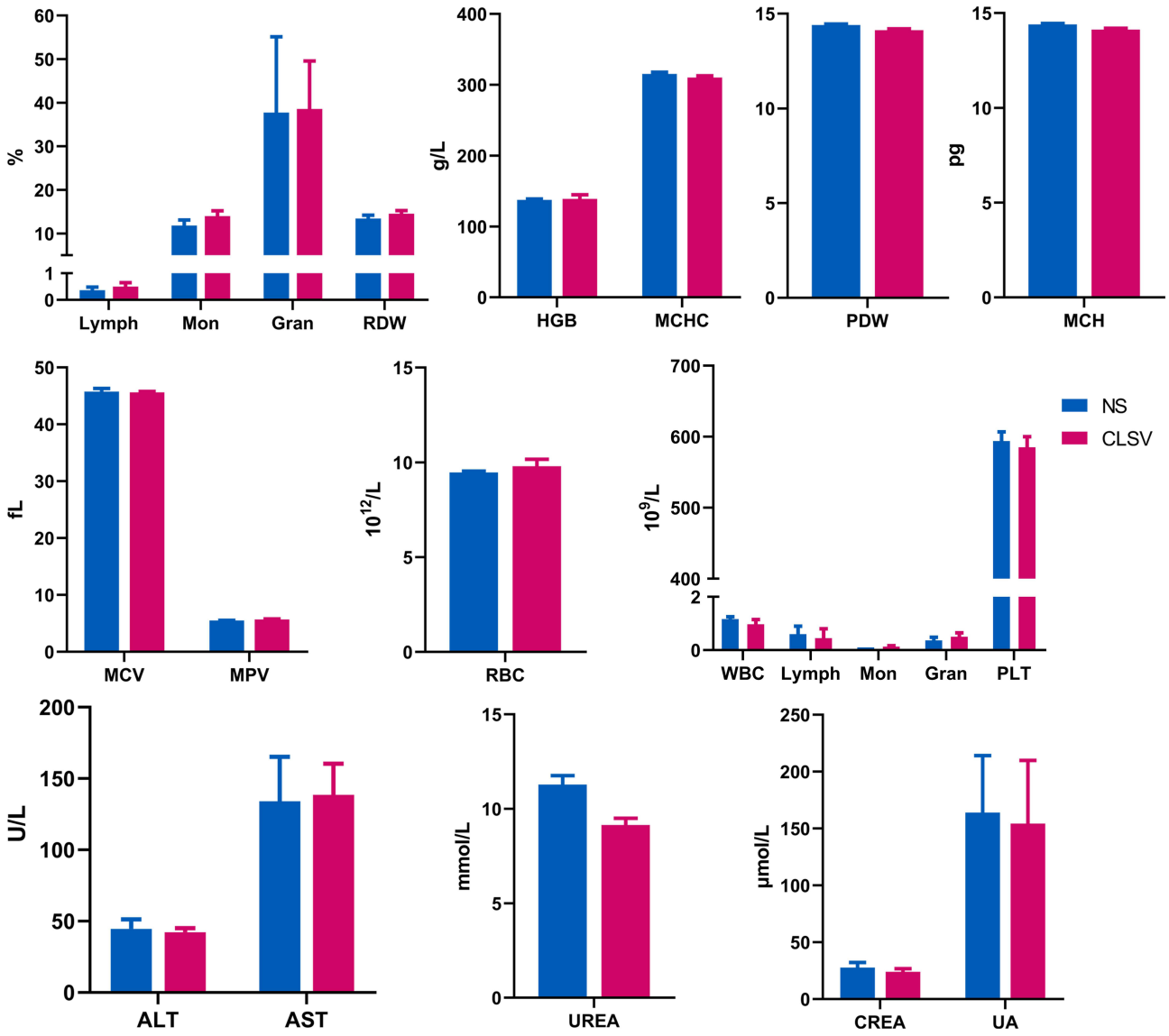

Figure 8 Blood biochemistry analysis and routine blood analysis of the toxicity of CLSV/IL-22BP complex by intravenous injection.

our results indicated that the CLSV/IL-22BP complex could induce anti-apoptosis, angiogenesis, and immune response to inhibit tumor cell growth in vivo with high safety.

Discussion

In our research, the IL-22BP encoded mRNA could be highly delivered by prepared CLSV system for colorectal cancer treatment. By encapsulating lysate into the internal DMP and surface modification of CPPs, the CLSV system reaches the dual purpose of activating immune response and enhancing mRNA delivery (Figure 9). According to our results, after the CLSV/IL-22BP complex treatment, the subcutaneous and intraperitoneal metastasis tumor models were significantly inhibited. Demonstrating that CLSV is a potential candidate vector for mRNA delivery, exhibiting great potential for cancer treatment.

Efficiency delivery of mRNA is critical to mRNA-based cancer treatment. Due to the liner and irregularly elongated mRNA, it is difficult to deliver. Currently, to development an ideal mRNA delivery vector, efforts have been made.[26] Such as Mai et al demonstrated that the mRNA is concentrated by protamine before encapsulation by DOTAP/Chol/DSPE-PEG cationic liposomes.[27] Palmiero et al showed the synthesis of PBAE terpolymer-based diacrylates and dodecyl

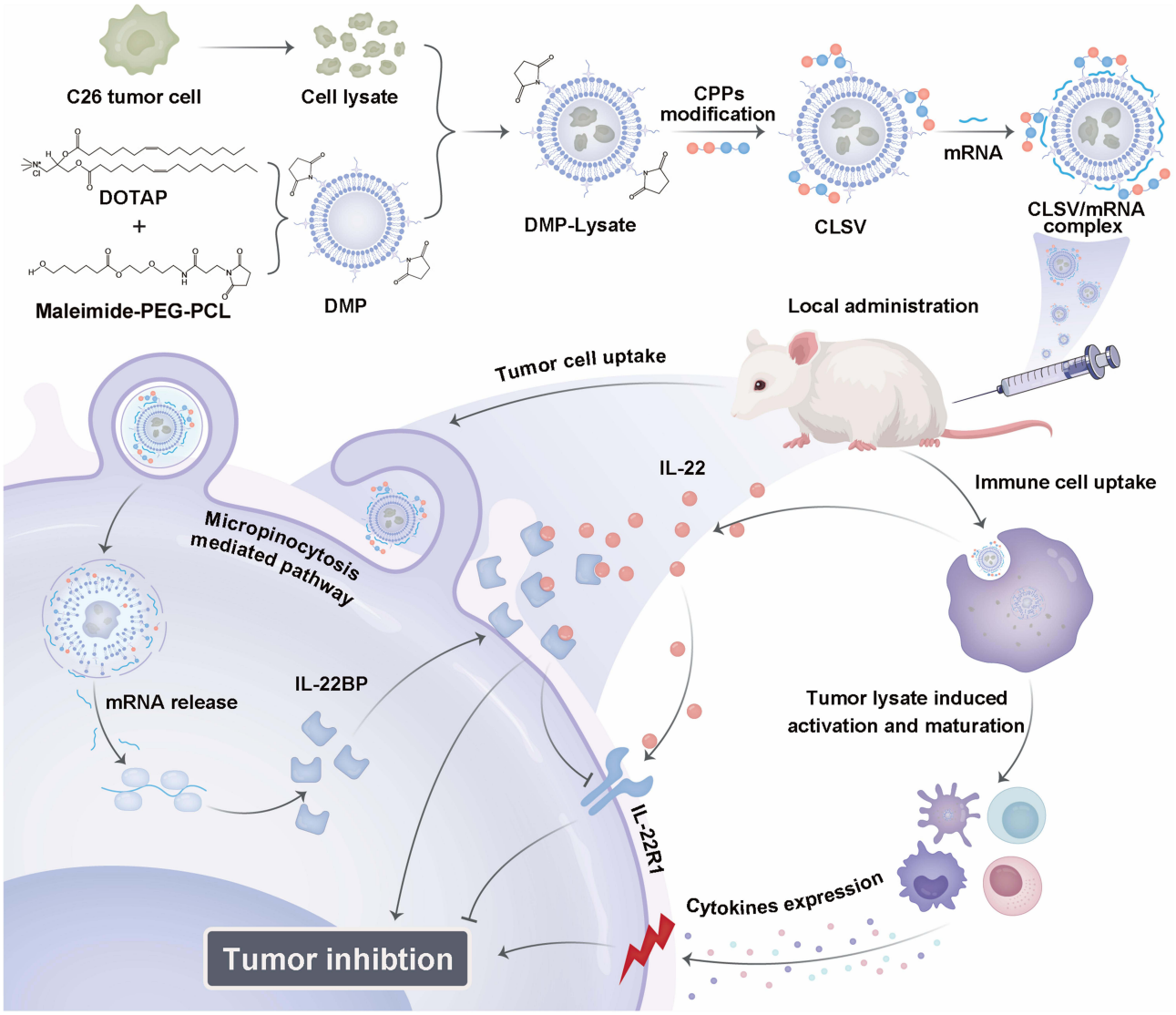

Figure 9 A schematic diagram of the prepared process and therapeutic process of the CLSV/IL-22BP complex.

amine to deliver mRNA to accumulate in the spleen.[28] Moreover, Miao et al used synthesized ionizable lipids, DOPE, cholesterol, and C14-PEG-2000 to construct the multi-component to deliver mRNA.[29] Currently, effort has been made in mRNA delivery, but some limitation needs to be solved. For example, the delivery efficiency of mRNA needs to be further enhanced and the "multi-vector system" needs to be simplified. In our study, we prepared a CLSV system that could deliver mRNA. When incubated with IL-22BP mRNA, the CLSV/IL-22BP complex exhibits highly tumor cell growth inhibition of 82.3% on clone formation. Our studies further show that the modification of CPPs can promote the uptake of mRNA via the micropinocytosis pathway. Moreover, the CLSV/IL-22BP complex exhibits a high tumor growth inhibition effect in subcutaneous (75.0%) and abdominal (84.9%). The advantages of the DMP skeleton may result in the highly efficient delivery of the CLSV system. Moreover, the modification of CPPs on the surface of DMP promotes the absorption of CLSV/IL-22BP complex by micropinocytosis pathway. Rapoport et al demonstrated that the mitochondrial enzymes can be delivered into mitochondria by TAT-LAD fusing protein, and it can effectively deliver in vivo.[30] Moreover, Saifi et al demonstrated that NPs coupled with iRGD exhibit highly effective anti-angiogenic ability by increasing cell uptake.[31] Research demonstrated that TAT-iRGD has strong cell absorption ability. Suggesting iRGD peptide could lead CLSV/IL-22BP complex into deeper tumor locations and inhibit tumor growth fundamentally.

Additionally, the steric hindrance form by CPPs modification. Which seems to reduce the likelihood of mRNA degradation from RNase A.

Immunogene therapy is one of the methods of cancer treatment.[32] However, the difficulty of the development of immunogene therapy is the lack of immune stimulation. Currently, researchers have been studies to deliver immune stimulation such as immune-stimulation gene and polysaccharides.[33] Indeed, Mendiratta et al reported that the expression of various immune cells including NK cells and T cells increased by delivery *IL-22* gene, resulting in the inhibition of tumor cell growth.[34] Denda-Nagai et al demonstrated that the antigens galactose and N-acetylgalactosamine (mMGL) were presented to bone marrow-derived immature DCs through C-type lectin in -vitro.[35] Wang et al demonstrated that TCL@PDA NPs were prepared by encapsulated tumor cell lysate into PDA NPs. Which can promote DC cell maturation and enhance the expression of Th1-related cytokines.[36] Currently, effort has been made in mRNA delivery, some limitation needs to be solved. There was too little nanomaterial-tumor cell lysate therapy to studies. In our paper, we study the immune stimulation effect of CLSV in vitro and in vivo. Firstly, the CLSV system increased DC maturation by up to 57.6% and the MHC II expression rate to 62.5% in vitro. Moreover, the CLSV system could enhance the maturation of DC and the expression of MHC II in vivo. According to our results, CLSV exhibits tumor growth inhibition effects in subcutaneous (45.7%) and abdominal (38.1%). Which indicated the high-efficiency inhibition of tumor cell growth potential of the CLSV system. The advantages of the DMP skeleton may result in the immune response ability and anticancer capacity of the CLSV system. Firstly, the abundant functional groups make it easy to introduce lysate into the DMP chain. Resulting in the slow release of lysate in vivo. Although there is no intact cell morphology in the tumor cell lysate of the CLSV system, the biomarkers remain. Currently, marketed multiple chemical inhibitors can downregulate PD-L1 expression in cells, direct regulatory signaling pathways associated with inducible PD-L1, and improve immunotherapy.[37] Moreover, the combination and immunosuppressants of PD-1 or PD-L1 inhibitors with cytotoxic chemotherapy or CTLA-4 antibodies is a potential cancer treatment manner.[38] Which gives us a lot of inspiration. The components of lysate such as intracellular protein and polysaccharide abundant in the biomarkers of lysate. Resulting in more stronger immune response and decreased immune escape. Moreover, the DMP skeleton has an abundant positive charge and specific epitope structure activation complement system, demonstrating a certain degree of immune response capacity. According to our results, compared to the DMP group and lysate group, the immune response effect of the CLSV system group was further increased. Which indicated that the adjuvant-like ability of DMP. However, which is the specific biomarkers recognized by DCs remain to be determined. In a word, the prepared CLSV system has potential value as an mRNA gene vector due to its low toxicity.

Conclusion

In our paper, we prepared a mRNA delivery vector named CLSV system. Which encapsulated tumor cell lysate on the DMP chain before modification of CPPs on the surface. The constructed CLSV reaches the double purpose of activation immunoreaction and enhance mRNA delivery. CLSV system, through binding IL-22BP mRNA forming CLSV/IL-22BP complex. Which exhibits potent tumor cell growth ability in vitro and in vivo. Our work indicated that CLSV represents a potential vector for mRNA delivery.

Acknowledgments

This work is supported by Medico-Engineering Cooperation Funds from the University of Electronic Science and Technology of China (ZYGX2021YGLH225), the Key Research Program of Science and Technology Department of Sichuan Province (2023YFS0165, 23NSFJQ0104) and the Science Foundation of Chengdu (2022-YF05-01793-SN).

Disclosure

The authors report no conflicts of interest.

References

1. Dolgin E. Cancer's new normal. *Nat Cancer*. 2021;2(12):1248–1250. doi:10.1038/s43018-021-00304-7
2. Shah SC, Itzkowitz SH. Colorectal cancer in inflammatory bowel disease: mechanisms and management. *Gastroenterology*. 2022;162(3):715–730 e713. doi:10.1053/j.gastro.2021.10.035
3. Mullard A. Addressing cancer's grand challenges. *Nat Rev Drug Discov*. 2020;19(12):825–826. doi:10.1038/d41573-020-00202-0
4. Wong-Rolle A, Wei HK, Zhao C, Jin C. Unexpected guests in the tumor microenvironment: microbiome in cancer. *Protein Cell*. 2021;12 (5):426–435. doi:10.1007/s13238-020-00813-8
5. Giamas G. Cancer Gene Therapy: vision and strategy for the new decade. *Cancer Gene Ther*. 2020;27(3–4):115. doi:10.1038/s41417-020-0169-8
6. Liu C, Shi Q, Huang X, Koo S, Kong N, Tao W. mRNA-based cancer therapeutics. *Nat Rev Cancer*. 2023;23(8):526–543. doi:10.1038/s41568-023-00586-2
7. Fabbri L, Chakraborty A, Robert C, Vagner S. The plasticity of mRNA translation during cancer progression and therapy resistance. *Nat Rev Cancer*. 2021;21(9):558–577. doi:10.1038/s41568-021-00380-y
8. Barbieri I, Kouzarides T. Role of RNA modifications in cancer. *Nat Rev Cancer*. 2020;20(6):303–322. doi:10.1038/s41568-020-0253-2
9. Papachristofilou A, Hipp MM, Klinkhardt U, et al. Phase Ib evaluation of a self-adjuvanted protamine formulated mRNA-based active cancer immunotherapy, BI1361849 (CV9202), combined with local radiation treatment in patients with stage IV non-small cell lung cancer. *J Immunother Cancer*. 2019;7(1):38. doi:10.1186/s40425-019-0520-5
10. Sahin U, Muik A, Derhovanessian E, et al. COVID-19 vaccine BNT162b1 elicits human antibody and T(H)1 T cell responses. *Nature*. 2020;586 (7830):594–599. doi:10.1038/s41586-020-2814-7
11. Chablani L, Singh V. Cell-penetrating peptides as passive permeation enhancers for transdermal drug delivery. *AAPS Pharm Sci Tech*. 2022;23 (7):266. doi:10.1208/s12249-022-02424-4
12. Khan MM, Filipczak N, Torchilin VP. Cell penetrating peptides: a versatile vector for co-delivery of drug and genes in cancer. *J Control Release*. 2021;330:1220–1228. doi:10.1016/j.jconrel.2020.11.028
13. Jhunjhunwala S, Hammer C, Delamarre L. Antigen presentation in cancer: insights into tumour immunogenicity and immune evasion. *Nat Rev Cancer*. 2021;21(5):298–312. doi:10.1038/s41568-021-00339-z
14. Blass E, Ott PA. Advances in the development of personalized neoantigen-based therapeutic cancer vaccines. *Nat Rev Clin Oncol*. 2021;18 (4):215–229. doi:10.1038/s41571-020-00460-2
15. van den Bulk J, Verdegaal EM, de Miranda NF. Cancer immunotherapy: broadening the scope of targetable tumours. *Open Biol*. 2018;8(6). doi:10.1098/rsob.180037
16. He J, Xiong X, Yang H, et al. Defined tumor antigen-specific T cells potentiate personalized TCR-T cell therapy and prediction of immunotherapy response. *Cell Res*. 2022;32(6):530–542. doi:10.1038/s41422-022-00627-9
17. Olivier T, Migliorini D. Autologous tumor lysate-loaded dendritic cell vaccination in glioblastoma: what happened to the evidence? *Rev Neurol*. 2023;179(5):502–505. doi:10.1016/j.neurol.2023.03.014
18. Gao Y, Men K, Pan C, et al. Functionalized DMP-039 hybrid nanoparticle as a novel mRNA vector for efficient cancer suicide gene therapy. *Int J Nanomed*. 2021;16:5211–5232. doi:10.2147/IJN.S319092
19. Li J, Men K, Gao Y, et al. Single micelle vectors based on lipid/block copolymer compositions as mRNA formulations for efficient cancer immunogene therapy. *Mol Pharm*. 2021;18(11):4029–4045. doi:10.1021/acs.molpharmaceut.1c00461
20. Lim C, Savan R. The role of the IL-22/IL-22R1 axis in cancer. *Cytokine Growth Factor Rev*. 2014;25(3):257–271. doi:10.1016/j.cytogfr.2014.04.005
21. Markota A, Endres S, Kobold S. Targeting interleukin-22 for cancer therapy. *Hum Vaccin Immunother*. 2018;14(8):2012–2015. doi:10.1080/21645515.2018.1461300
22. Lei S, Zhang X, Men K, et al. Efficient colorectal cancer gene therapy with IL-15 mRNA nanoformulation. *Mol Pharm*. 2020;17(9):3378–3391. doi:10.1021/acs.molpharmaceut.0c00451
23. Zhang X, Cai A, Gao Y, Zhang Y, Duan X, Men K. Treatment of melanoma by nano-conjugate-delivered Wee1 siRNA. *Mol Pharm*. 2021;18 (9):3387–3400. doi:10.1021/acs.molpharmaceut.1c00316
24. Macri C, Pang ES, Patton T, O'Keeffe M. Dendritic cell subsets. *Semin Cell Dev Biol*. 2018;84:11–21. doi:10.1016/j.semcdb.2017.12.009
25. Sadeghzadeh M, Bornehdeli S, Mohahammadrezakhani H, et al. Dendritic cell therapy in cancer treatment; the state-of-The-art. *Life Sci*. 2020;254:117580. doi:10.1016/j.lfs.2020.117580
26. Oberli MA, Reichmuth AM, Dorkin JR, et al. Lipid nanoparticle assisted mRNA delivery for potent cancer immunotherapy. *Nano Lett*. 2017;17 (3):1326–1335. doi:10.1021/acs.nanolett.6b03329
27. Mai Y, Guo J, Zhao Y, Ma S, Hou Y, Yang J. Intranasal delivery of cationic liposome-protamine complex mRNA vaccine elicits effective anti-tumor immunity. *Cell Immunol*. 2020;354:104143. doi:10.1016/j.cellimm.2020.104143
28. Capasso Palmiero U, Kaczmarek JC, Fenton OS, Anderson DG. Poly(beta-amino ester)-co-poly(caprolactone) Terpolymers as nonviral vectors for mRNA delivery in vitro and in vivo. *Adv Healthc Mater*. 2018;7(14):e1800249. doi:10.1002/adhm.201800249
29. Miao L, Li L, Huang Y, et al. Delivery of mRNA vaccines with heterocyclic lipids increases anti-tumor efficacy by STING-mediated immune cell activation. *Nat Biotechnol*. 2019;37(10):1174–1185. doi:10.1038/s41587-019-0247-3
30. Rapoport M, Saada A, Elpeleg O, Lorberboum-Galski H. TAT-mediated delivery of LAD restores pyruvate dehydrogenase complex activity in the mitochondria of patients with LAD deficiency. *Mol Ther*. 2008;16(4):691–697. doi:10.1038/mt.2008.4
31. Saifi MA, Sathish G, Bazaz MR, Godugu C. Exploration of tumor penetrating peptide iRGD as a potential strategy to enhance tumor penetration of cancer nanotherapeutics. *Biochim Biophys Acta Rev Cancer*. 2023;1878(3):188895. doi:10.1016/j.bbcan.2023.188895
32. Ott PA, Hu Z, Keskin DB, et al. An immunogenic personal neoantigen vaccine for patients with melanoma. *Nature*. 2017;547(7662):217–221. doi:10.1038/nature22991
33. Andrejeva G, Rathmell JC. Similarities and distinctions of cancer and immune metabolism in inflammation and tumors. *Cell Metab*. 2017;26 (1):49–70. doi:10.1016/j.cmet.2017.06.004
34. Mendiratta SK, Quezada A, Matar M, et al. Intratumoral delivery of IL-12 gene by polyvinyl polymeric vector system to murine renal and colon carcinoma results in potent antitumor immunity. *Gene Ther*. 1999;6(5):833–839. doi:10.1038/sj.gt.3300891

35. Denda-Nagai K, Kubota N, Tsuiji M, Kamata M, Irimura T. Macrophage C-type lectin on bone marrow-derived immature dendritic cells is involved in the internalization of glycosylated antigens. *Glycobiology*. 2002;12(7):443–450. doi:10.1093/glycob/cwf061
36. Wang X, Wang N, Yang Y, et al. Polydopamine nanoparticles carrying tumor cell lysate as a potential vaccine for colorectal cancer immunotherapy. *Biomater Sci*. 2019;7(7):3062–3075. doi:10.1039/c9bm00010k
37. Wu Y, Chen W, Xu ZP, Gu W. PD-L1 distribution and perspective for cancer immunotherapy-blockade, knockdown, or inhibition. *Front Immunol*. 2019;10:2022. doi:10.3389/fimmu.2019.02022
38. Ghosh C, Luong G, Sun Y. A snapshot of the PD-1/PD-L1 pathway. *J Cancer*. 2021;12(9):2735–2746. doi:10.7150/jca.57334

International Journal of Nanomedicine Dovepress

Publish your work in this journal

The International Journal of Nanomedicine is an international, peer-reviewed journal focusing on the application of nanotechnology in diagnostics, therapeutics, and drug delivery systems throughout the biomedical field. This journal is indexed on PubMed Central, MedLine, CAS, SciSearch®, Current Contents®/Clinical Medicine, Journal Citation Reports/Science Edition, EMBase, Scopus and the Elsevier Bibliographic databases. The manuscript management system is completely online and includes a very quick and fair peer-review system, which is all easy to use. Visit http://www.dovepress.com/testimonials.php to read real quotes from published authors.

Submit your manuscript here: https://www.dovepress.com/international-journal-of-nanomedicine-journal